Matrix-Isolation FTIR Spectroscopy of Benzil: Probing the Flexibility of the C−C Torsional Coordinate

S. Lopes,[†] A. Gómez-Zavaglia,[†,‡] L. Lapinski,[§] N. Chattopadhyay,[||] and R. Fausto*[,†]

Department of Chemistry, University of Coimbra, P-3004−535, Portugal, Faculdad de Farmacia y Bioquímica, Universidad de Buenos Aires, Buenos Aires, Argentina, Institute of Physics, Polish Academy of Sciences, Al. Lotnikow 32/46, 02-668 Warsaw, Poland, and Department of Chemistry, Jadavpur University, Calcutta 700 032, India

Received: July 1, 2004; In Final Form: August 2, 2004

The infrared spectrum and conformational flexibility of benzil, $(C_6H_5CO)_2$, are studied by matrix-isolation FTIR spectroscopy, supported by DFT calculations. It is shown that the low-frequency (ca. 25 cm^{-1}), large-amplitude torsion around the C−C central bond strongly affects the structural and spectroscopic properties exhibited by the compound. The equilibrium conformational distribution of molecules with different O═C−C═O dihedral angles, existing at room temperature in the gas phase, and trapped in a low-temperature ($T = 9$ K) inert matrix can be changed either by in situ irradiation with UV light ($\lambda > 235$ nm) or by annealing the matrix to higher temperatures ($T \approx 34$ K). In the first case, the increase of the average O═C−C═O angle results from conformational relaxation in the excited electronic states (S_1 and T_1), whose lowest-energy conformations correspond, for both S_1 and T_1 states, to a nearly planar configuration with the O═C−C═O dihedral angle equal to 180°. In the second case, the decrease of the average value of the O═C−C═O dihedral angle is a consequence of the change in the S_o C−C torsional potential, resulting from interactions with the matrix media, which favors the stability of the more polar structures with smaller O═C−C═O dihedral angles.

Introduction

α-Dicarbonyl compounds have been the subject of extensive research because of their important practical applications.[1−4] Among them, diaromatic α-dicarbonyls, such as benzil $[(C_6H_5CO)_2]$,[72] which was synthesized for the first time by Laurent in 1835,[5] are important for their photorotamerism.[6−18] Benzil is also a known intermediate for organic synthesis and is currently used as a UV hardening agent and a pesticide.[19] It has also received considerable interest because of its unusual optical and structural properties in the solid phases.[16,19−22]

The gaseous phase of benzil was studied by electron diffraction at 448 K.[23] That study concluded on the existence of a single, doubly degenerated-by-symmetry conformer in the gas phase, where the O═C−C═O torsion angle is ca. ±117° and the phenyl rings are nearly coplanar with the carbonyl groups (Figure 1).

As in other α-dicarbonyl compounds (e.g., diacetyl, $(CH_3CO)_2$),[24−27] the movement along the τC−C torsional coordinate in benzil corresponds to a low-frequency, large-amplitude vibration, which can be expected to be of particular importance in determining the conformational, structural, and vibrational properties of the molecule. The average value for the O═C−C═O dihedral angle can then be expected to be strongly determined by temperature and phase and be extremely sensitive to the chemical environment.

It is consensually accepted that the conformational preferences of α-dicarbonyl compounds in the gaseous phase result mainly from the balance between steric and resonance effects. The latter are maximized in the planar configurations, whereas steric effects, which result from interactions between the carbonyl oxygens and/or the substituents at the carbonyl carbon atom, favor nonplanar structures. These effects have been found to be strongly dependent on the electronic state: in benzil, for example, contrary to what succeeds in the ground electronic state (S_o), the most stable conformation of the O═C−C═O axis in both the T_1 and S_1 excited states corresponds to a nearly planar trans configuration.[6−17]

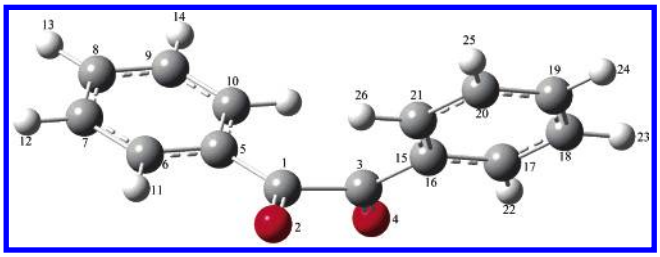

Figure 1. Minimum-energy conformation of benzil (C_2 symmetry; O═C−C═O dihedral angle: 116.6°) with atom numbering.

Previous theoretical studies of benzil confirmed the flexibility of the molecule with respect to the τC−C torsional coordinate. For the S_o state, calculations undertaken at different levels of theory[6,28−31] agree on the existence in the potential-energy surface of two symmetrically related, nonplanar minima with C_2 symmetry, thus confirming the electron diffraction results of Shen and Hagen.[23] Also in consonance with experimental data extracted from vibrational spectra and dipolar measurements,[30,32] the average equilibrium value of the O═C−C═O torsional angle was predicted to depend on the polarity of the media,[30,33] the dihedral angle becoming smaller when the polarity of the solvent increases (i.e., conformations with larger

* Corresponding author. E-mail: rfausto@ci.uc.pt.
[†] University of Coimbra.
[‡] Universidad de Buenos Aires.
[§] Polish Academy of Sciences.
[||] Jadavpur University.

10.1021/jp047116s CCC: $27.50
Published on Web 09/09/2004

dipole moments become stabilized in more polar chemical environments).

Theoretical studies on the excited states of benzil are very scarce. To the best of our knowledge, no ab initio or DFT studies dealing with this subject have been reported hitherto. A semiempirical (AM1; CNDO/S-CI) study of the S_1 and T_1 low-lying excited states' potential-energy surfaces of benzil[6] predicted that both states should have a trans planar global minimum. These results are consistent with previously reported experimental data[7,10−17] and have been confirmed since then by subsequent and more sophisticated experimental studies.[8,9] Nanosecond time-resolved infrared spectroscopy and picosecond time-resolved Raman spectroscopic investigations of benzil in carbon tetrachloride and cyclohexane solutions[9] lead to the conclusion that after photoexcitation the S_1 state shows an ultrafast conformational change to the trans planar geometry, accompanied by the shortening of the C═O bond lengths and the stretching of the C−C central bond. Intersystem crossing to the T_1 state can then take place on a time scale of a few nanoseconds. The T_1 state directly recovers back to the nonplanar S_o state.[9]

The vibrational spectra of benzil in the condensed phases (such as neat solid, molten phases, and solutions) were extensively studied in the past by a variety of different methods, including FTIR, Raman, circular dichroism, and Brillouin spectroscopies.[34−47] The great interest for the studies performed on the solid state have been motivated by the fact that benzil exhibits polymorphism, with the low-temperature phase (existing below ca. 83 K) presenting particularly interesting structural, electrical, and mechanical properties.[20,48−58] However, to the best of our knowledge, no vibrational spectroscopic studies have been performed on gaseous benzil or for the compound isolated in a low-temperature inert matrix.

The advantages of applying the matrix-isolation technique to the study of the conformational flexibility of benzil rely on the fact that the conformational equilibrium composition of the gas phase can be efficiently trapped in the matrixes,[59,60] thus being easily studied by conventional (non-time-resolved) FTIR spectroscopy. Because the spectral resolution under the matrix-isolation experimental conditions is greatly enhanced when compared with those attained in solution or crystalline phases, subtle features of the spectral parameters could be examined in detail and correlated with structural parameters, in particular, with the flexible torsional coordinate. However, the spectral bands observed under these conditions do not exhibit rotational structure (as expected for spectra obtained in the gaseous phase). Hence, the spectra of matrix-isolated species can be easily correlated with pure vibrational spectra that were obtained from theoretical calculations. Furthermore, both annealing and in situ irradiation experiments can be undertaken in the matrixes, enabling us to examine the effects of thermal relaxation in the ground electronic state potential-energy surface (and the influence of the matrix media on this surface) or in the low-lying excited states' potential-energy surfaces, respectively, as will be described in detail in this article.

Materials and Methods

Infrared Spectroscopy. Benzil was obtained from Aldrich and further purified by sublimation, followed by recrystallization from ethanol prior to spectra collection. The IR spectra were obtained using a Mattson (Infinity 60AR Series) Fourier transform infrared spectrometer equipped with a deuterated triglycine sulfate (DTGS) detector and a Ge/KBr beam splitter with 0.5-cm^{-1} spectral resolution. Necessary modifications of the sample compartment of the spectrometer were done to accommodate the cryostat head and allow for the purging of the instrument by a stream of pretreated dry air to remove water vapor and CO_2. A solid sample of benzil was placed in a specially designed doubly thermostattable Knudsen cell.[59] Both the sample container and valve nozzle compartments of this cell were kept at 353 K. Matrixes were prepared by codeposition of benzil vapors coming out of the Knudsen cell together with a large excess of the matrix gas (argon N60, obtained from Air Liquide) onto the CsI substrate of the cryostat cooled to 9 K. Care was taken to keep the guest-to-host ratio in matrixes low enough to avoid association. All experiments were performed using an APD Cryogenics close-cycle helium refrigeration system with a DE-202A expander, and in all cases, the deposition temperature was 9 K.

Irradiation of the matrixes was undertaken through the outer KBr window of the cryostat ($\lambda > 235$ nm) with unfiltered light from a 150-W xenon arc lamp (Osram XBO 150W/CR OFR).

Computational Methodology. The quantum chemical calculations were performed with Gaussian 98 (revision A.9)[61] at the DFT level of theory using the 6-31G(d,p) and 6-311++G(d,p) basis sets and the three-parameter density functional abbreviated as B3LYP, which includes Becke's gradient exchange correction[62] and the Lee, Yang, Parr correlation functional.[63]

Geometrical parameters of the considered conformations were optimized at each level of theory using the geometry direct inversion of the invariant subspace (GDIIS) method.[64] To assist with the analysis of the experimental spectra, vibrational frequencies and IR intensities were also calculated with the two basis sets. The computed harmonic frequencies were scaled down by a single factor (0.978) to correct them for the effects of basis set limitations, the neglected part of electron correlation, and anharmonicity effects. Potential-energy torsional profiles were obtained with both the 6-31G(d,p) and 6-311++G(d,p) basis sets. In these calculations, all geometrical parameters except for the O═C−C═O torsional angle (fixed at a given value, using increments of 30°) were optimized. The energy-weighted average O═C−C═O dihedral angles and dipole moments, at a given temperature, were estimated using a simple classical model that takes into consideration all significantly populated conformations differing in the O═C−C═O torsional angle. The applied procedure follows the method previously described by Gómez-Zavaglia and Fausto.[24] Normal coordinate analysis was undertaken in the internal coordinates space, as described by Schachtschneider,[65] using the program BALGA and the optimized geometries and harmonic force constants resulting from the DFT(B3LYP)/6-311++G(d,p) calculations. Effects of media were estimated by using the polarized continuum model (PCM).[66]

Results and Discussion

Geometries and Energies. The potential-energy profile for internal rotation around the C−C central bond in benzil, calculated in the present study at the DFT(B3LYP)/6-311++G(d,p) level of approximation, is shown in Figure 2. In agreement with the accumulated information on the conformational preferences of benzil in its ground electronic state, the calculations predicted the existence of a doubly degenerated-by-symmetry minimum of C_2 symmetry with nonplanar geometry. At the applied level of theory, the O═C−C═O dihedral angle in the minimum-energy conformations is predicted to be equal to ±116.6°.

The comparison between the calculated geometries and the experimental structural parameters obtained for the molecule

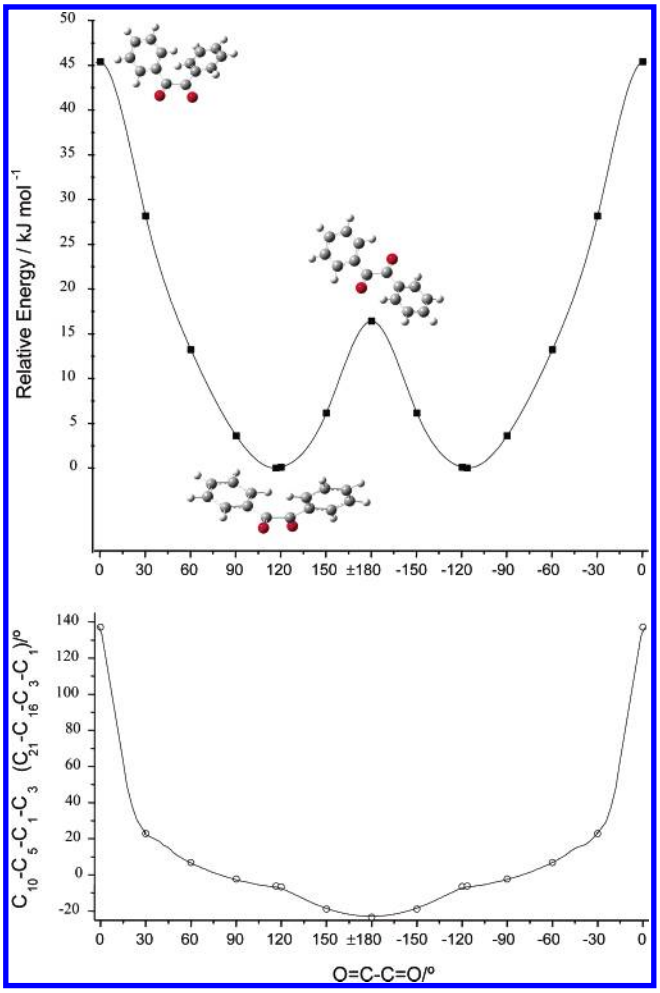

Figure 2. DFT(B3LYP)/6-311++G(d,p)-calculated conformational relative energies (-■-) and $C_{10}-C_5-C_1-C_3$ ($C_{21}-C_{16}-C_3-C_1$) dihedral angles (-○-) as a function of the O=C−C=O dihedral angle.

in the gaseous phase (electron-diffraction data[23]) is given in Supporting Information, Table S1. The geometry previously obtained for the solid compound by X-ray crystallography[20,22,48] is also shown in this Table. Although a few calculated structural parameters that were obtained with the two basis sets used in this study differ somewhat, in general terms, both calculations adequately reproduce the experimental geometries with those obtained with the largest basis set [6-311++G(d,p)] showing the best agreement with the experimental data. In particular, the present calculations give additional theoretical support to the observation that the C−C central bond is longer than the two $C-C_\alpha$ bonds. The lengths of these bonds calculated using the 6-311++G(d,p) basis set are 154.4 and 148.7 pm, respectively. These values agree very well with the corresponding experimental bond lengths of 154.6 and 148.8 pm.[23] The length of the C−C central bond in benzil is typical of a nonconjugated carbon−carbon bond, and it results from the balance between the relatively weak π-electron delocalization within the O=C−C=O moiety (which tends to shorten this bond length) and the more important σ-electron system repulsion due to the interaction between the positively charged carbonyl carbon atoms (which tends to increase the carbon−carbon distance). A similar, although less pronounced, situation has been previously observed for diacetyl, where the equivalent bond lengths were found to be 153.0 and 151.5 pm, respectively.[24,67] We note that the 6-311++G(d,p) calculated value for the O=C−C=O dihedral angle in benzil is practically equal to that obtained by electron diffraction (116.9°[23]). It must, however, be pointed out that the experimental geometry obtained by electron diffraction is affected by vibrational contributions. Because the τC−C torsional vibration corresponds to a large-amplitude vibration (its calculated frequency is only 26 cm^{-1}), it is not possible to make conclusions, on the basis of only this result, about the ability of the theoretical calculations to predict the equilibrium value for the O=C−C=O dihedral angle.

The heights of two energy barriers to torsion around the central C−C bond have been calculated at the DFT(B3LYP)/6-311++G(d,p) level. The barrier that has its top at 180° was predicted to be of moderate height, 16.4 kJ mol^{-1} (11.7 kJ mol^{-1} with the 6-31G(d,p) basis set), whereas the barrier that has its top at 0° should, according to the calculations, be considerably higher, 45.4 kJ mol^{-1} (48.2 kJ mol^{-1} with the 6-31G(d,p) basis set). This result could be expected because for the 0° conformation the repulsions between the two phenyl groups, on one side of the molecule, and between the oxygen lone electron pairs, on the other side, should be significantly stronger in comparison to the corresponding interactions in the 180° conformation. Despite this, the potential energy increases faster when the system changes from the minimum-energy conformation toward the 180° conformation than when it changes toward the 0° conformation (compare, for example, the energies corresponding to the O=C−C=O values at 90 and 150°, Figure 2). Assuming a model where the large-amplitude, low-frequency torsion around the central C−C bond is treated classically and calculating the number of molecules of benzil with a given conformation around the central C−C bond from the Boltzmann distribution, the energy-weighted dihedral angle can be estimated from eq 1

$$|\alpha| = \int_{-180^\circ}^{180^\circ} |\alpha| N(\alpha)\, d\alpha \qquad (1)$$

where α is the O=C−C=O dihedral angle ($\alpha \in [-180°, 180°]$) and $N(\alpha)$ is the fractional population of molecules with the O=C−C=O dihedral equal to α, which is given by

$$N(\alpha) = \frac{e^{-E(\alpha)/RT}}{\int_{-180^\circ}^{180^\circ} e^{-E(\alpha)/RT}\, d\alpha} \qquad (2)$$

Numerical integration of eq 1, using the relative energies calculated at the DFT(B3LYP)/6-311++G(d,p) level of theory (Figure 2), gives an estimate of the energy-averaged O=C−C=O dihedral angle at room temperature (T = 298 K) of 116.1°, being slightly smaller than the equilibrium angle (116.6°). For the temperature of the nozzle used in this study, the calculations yield an energy-averaged dihedral angle of 115.9°, whereas for the temperature used in the electron-diffraction experiment (448 K[23]), the calculated value is 115.5°, which is still a fairly good estimate of the experimental value (116.9°[23]).

A slight modification of eq 1 enables us to determine the energy-weighted average deviations of the O=C−C=O dihedral angle from equilibrium in both O=C−C=O increasing and decreasing directions. (To do this, it is only necessary to change the integration interval to the appropriated regions of positive and negative deviations of the dihedral angle from the equilibrium, and renormalize the weighting function appropriately.) The deviations (smaller dihedral/larger dihedral) change from (12.7:12.2°) for room temperature to (13.6:12.8°) and (15.6:13.8°) for T = 353 and 448 K, respectively.

Figure 3 shows the $N(\alpha)$ function for T = 9, 298, 353, and 448 K (superimposed with the potential-energy profile for rotation around the C−C central bond). It is clear from this Figure that although the average value of the O=C−C=O

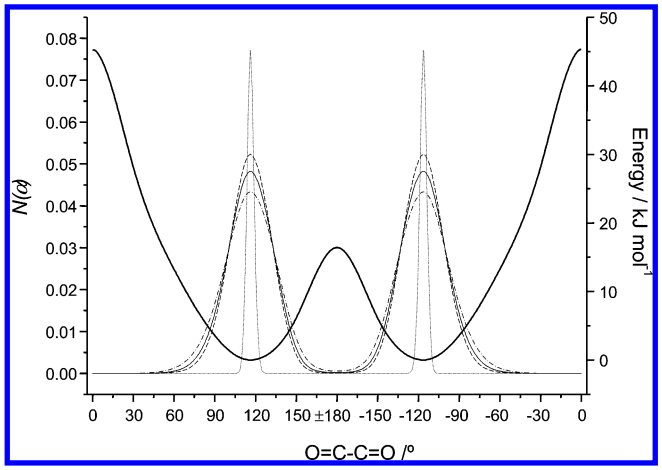

Figure 3. DFT(B3LYP)/6-311++G(d,p)-calculated potential-energy profile for internal rotation around the central C−C bond of benzil (—) and energy-weighted fractional conformational populations (estimated accordingly to the Boltzmann distribution) for $T = 9$ (···), 298 (- - -), 353 (—), and 448 (-·-·-) K.

dihedral angle is not much affected by the temperature (due to the nearly symmetrical shape of the potential around the minima), for all but the lowest temperature considered, the fraction of molecules existing in thermodynamic equilibrium with a O═C−C═O dihedral angle significantly smaller or larger than its equilibrium value is substantial. It can then be easily anticipated that this fact shall manifest itself clearly in the vibrational spectra of benzil. We shall return to this point further below.

Figure 2 also shows the variation of the $C_{10}-C_5-C_1-C_3$ and $C_{21}-C_{16}-C_3-C_1$ dihedral angles with the O═C−C═O torsion, which expresses the deviation of the phenyl (ϕ) groups from the planes defined by the carbonyl moieties. These angles were found to be nearly 0° for conformations around the minima and to deviate considerably from this value for conformations approaching both the cis and trans configurations of the O═C−C═O axis, a result that can be rationalized considering a balance between the π stabilization of planar O═C−ϕ structures and the favoring of nonplanar geometries because of steric strain in the molecule. It becomes clear from this picture that the minimum-energy conformations correspond to a situation where the steric strain is minimal, enabling maximization of the π-stabilization effect in the O═C−ϕ fragments. (This occurs at expense of losing π stabilization in the O═C−C═O fragment.)

The influence of the large-amplitude, low-frequency τC−C torsional vibration on the dipole moment of benzil could also be expected to be considerable because the dependence of the dipole moment on the value of the O═C−C═O dihedral angle is very large. The dipole moment is equal to zero in the planar trans conformation and attains its maximum value for a value of the O═C−C═O dihedral close to 0° (6.12 D; 6-311++G(d,p) calculated value; Figure 4). However, the energy-weighted calculated average dipole moment[73] was not found to differ in practical terms from the equilibrium value, 3.46 D (6-311++G(d,p) value, which agrees very closely with the experimentally reported value of the dipole moment of benzil in cyclohexane solution, 3.48 D[68]), at all temperatures studied (9, 298, 353, and 448 K).

Vibrational Spectra. The benzil molecule has 72 fundamental vibrations, spanning the representation 37A + 35B, with both A and B symmetry-type vibrations being active in the infrared. The 54 internal phenyl vibrations correspond to in-

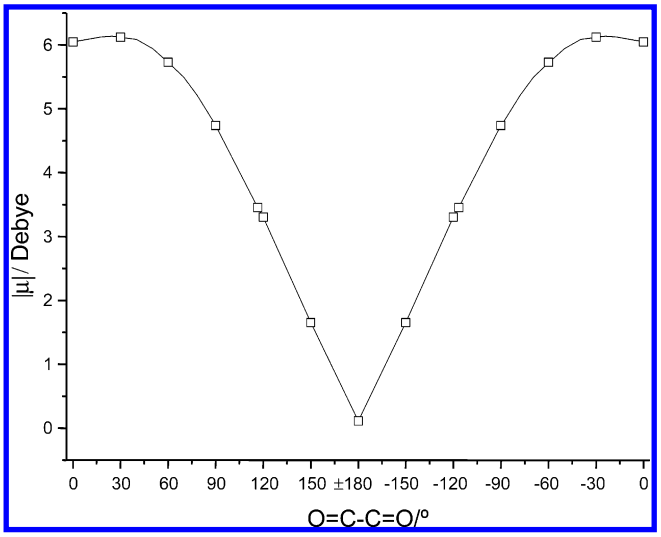

Figure 4. DFT(B3LYP)/6-311G(d,p)-calculated dipole moment of benzil as a function of the O═C−C═O dihedral angle.

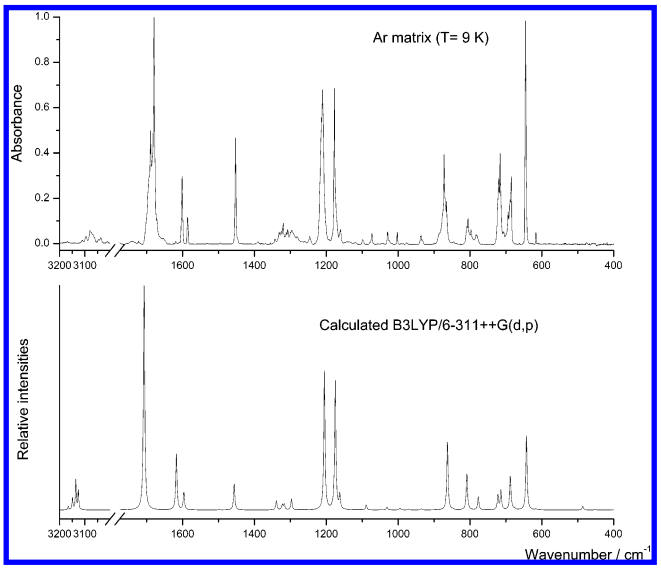

Figure 5. Infrared spectrum of benzil in an argon matrix (substrate temperature = 9 K; nozzle temperature = 353 K) and DFT(B3LYP)/6-311++G(d,p)-calculated spectrum for the minimum-energy conformation. Calculated spectrum was simulated using Lorentzian functions centered on the calculated (scaled) frequency with the bandwidth at half-height equal to 5 cm^{-1}.

phase (A) and out-of-phase (B) motions involving the two phenyl groups; eight vibrations (5A and 3B) are localized in the bicarbonyl part of the molecule, forming three pairs of in-phase/out-of-phase modes plus two extra A-type vibrations (the C_1-C_3 stretching and torsional modes); the remaining five pairs of in-phase/out-of-phase modes (5A and 5B) are associated with vibrations involving the motion of the phenyl groups relative to the bicarbonyl moiety. The full definition of symmetry coordinates that were adopted in the vibrational analysis is provided in Table S2 (Supporting Information). The DFT-calculated [6-311++G(d,p)] spectrum and potential-energy distribution resulting from normal-mode analysis for the minimum-energy C_2 symmetry conformation are presented in Table S3 (Supporting Information).

The spectrum of benzil isolated in argon (substrate temperature, 9 K; nozzle temperature, 353 K) is presented in Figure 5, together with the calculated spectrum. The general assignment of the fundamental bands is straightforward and strongly facilitated by the excellent agreement between the observed and

TABLE 1: Experimental and Calculated Vibrational Data, and Results of Normal Coordinate Analysis for Benzil[a]

Approximate Description		Calculated wave-number[b]	Intensity	Experimental Ar Matrix wavenumber	Intensity[d]	PED[c]
ν(C-H 1) s	A	3135	2.3	3110	w	$S_{18}(45)$, $S_{20}(32)$, $S_{22}(10)$, $S_{24}(10)$
ν(C-H 1) as	B	3135	4.1			$S_{19}(45)$, $S_{21}(32)$, $S_{23}(10)$, $S_{25}(10)$
ν(C-H 2) s	A	3128	0.1	3095	w	$S_{18}(39)$, $S_{20}(46)$, $S_{24}(12)$
ν(C-H 2) as	B	3128	17.8			$S_{19}(38)$, $S_{21}(46)$, $S_{25}(11)$
ν(C-H 3) s	A	3118	4.2	3080/3074	w/w	$S_{18}(16)$, $S_{22}(62)$, $S_{26}(20)$
ν(C-H 3) as	B	3118	22.5			$S_{19}(16)$, $S_{23}(62)$, $S_{27}(20)$
ν(C-H 4) s	A	3109	1.3	3069/3062	w/w	$S_{20}(20)$, $S_{24}(78)$
ν(C-H 4) as	B	3109	16.9			$S_{21}(20)$, $S_{25}(78)$
ν(C-H 5) s	A	3097	0.3	3046/3037	w/w	$S_{22}(23)$, $S_{26}(76)$
ν(C-H 5) as	B	3097	0.4			$S_{23}(23)$, $S_{27}(76)$
ν(C=O) s	A	1689	129.7	1702,1700 /1697/1694/1692/	S	$S_2(87)$
ν(C=O) as	B	1689	300.7	1689 1686/1684/1680/1671[e]		$S_3(93)$
ν(C-C ring 2) as	B	1600	69.2	1601	m	$S_9(65)$, $S_{35}(10)$, $S_{58}(21)$
ν(C-C ring 2) s	A	1600	20.8			$S_8(65)$, $S_{34}(10)$, $S_{57}(21)$
ν(C-C ring 4) s	A	1582	5.6	1586	w	$S_{12}(66)$, $S_{55}(17)$
ν(C-C ring 4) as	B	1581	20.3			$S_{13}(66)$, $S_{56}(17)$
δ(C-H 2) as	B	1487	0.9	1494	w	$S_{15}(32)$, $S_{54}(64)$
δ(C-H 2) s	A	1487	0.7			$S_{14}(32)$, $S_{53}(62)$
δ(C-H 3) s	A	1446	0.3	1457/1452/1446	sh/m/w	$S_{16}(36)$, $S_{51}(18)$, $S_{55}(29)$
δ(C-H 3) as	B	1445	34.2			$S_{17}(36)$, $S_{52}(19)$, $S_{56}(29)$, $S_{60}(10)$
δ(C-H 3) as	B	1327	8.4	1343/1331	w/w	$S_{11}(20)$, $S_{17}(11)$, $S_{52}(55)$
δ(C-H 3) s	A	1327	0.0			$S_{10}(17)$, $S_{16}(10)$, $S_{51}(59)$
ν(C-C ring 3) s	A	1313	11.6	1326/1324/1320	sh/w/w	$S_{10}(62)$, $S_{51}(18)$
ν(C-C ring 3) as	B	1308	10.0	1311/1307	w/w	$S_{11}(67)$, $S_{52}(24)$
ν(C-C_α) s	A	1279	25.9	1299/1296/1293/1290/1282 1279/1266/1254/1245/1239[f]	m	$S_1(16)$, $S_4(36)$, $S_{42}(10)$
ν(C-C_α) as	B	1198	180.4	1218/1214/1213/1211/1208	S	$S_5(33)$, $S_7(12)$, $S_9(11)$, $S_{31}(11)$, $S_{58}(15)$
δ(C-H 4) s	A	1179	1.4	1183	w	$S_8(24)$, $S_{57}(73)$
δ(C-H 4) as	B	1170	152.5	1177/1173/1170	S	$S_9(13)$, $S_{58}(53)$
δ(C-H 5) s	A	1159	0.5	1164	w	$S_{10}(12)$, $S_{55}(13)$, $S_{59}(65)$
δ(C-H 5) as	B	1158	21.5	1160	m	$S_{11}(11)$, $S_{56}(13)$, $S_{60}(57)$
ν(C-C ring 6) s	A	1083	0.8	1099/1073[g]	w	$S_{16}(49)$, $S_{55}(31)$, $S_{59}(10)$
ν(C-C ring 6) as	B	1083	8.3			$S_{17}(52)$, $S_{56}(32)$, $S_{60}(10)$
ν(C-C ring 5) s	A	1041	0.8	1042	w	$S_1(14)$, $S_{14}(40)$, $S_{53}(20)$
ν(C-C ring 5) as	B	1024	5.8	1029	w	$S_7(15)$, $S_{15}(53)$, $S_{54}(23)$
δ(ring 1) s	A	1017	0.8	1025/1021	w/w	$S_6(26)$, $S_{14}(20)$, $S_{30}(33)$
δ(ring 1) as	B	994	4.1	1002	w	$S_7(42)$, $S_{31}(57)$
ν(C-C ring 1) s	A	994	0.1			$S_6(52)$, $S_{30}(46)$
γ(C-H 5) as	B	988	0.0	989/985	w	$S_{37}(25)$, $S_{70}(60)$
γ(C-H 5) s	A	988	0.0			$S_{36}(25)$, $S_{69}(61)$
γ(C-H 4) as	B	976	0.4	976/972	w	$S_{41}(22)$, $S_{68}(62)$
γ(C-H 4) s	A	976	0.4			$S_{40}(23)$, $S_{67}(64)$
γ(C-H 3) as	B	938	1.8	938/936	w/w	$S_{39}(11)$, $S_{66}(65)$
γ(C-H 3) s	A	934	1.3	933	w	$S_{38}(11)$, $S_{65}(72)$
ν(C-C ring 1) as	B	865	90.0	886/877/872/867/864	m	$S_7(12)$, $S_{29}(23)$, $S_{43}(18)$
γ(C-H 2) s	A	842	0.4	846/837	w	$S_{63}(99)$
γ(C-H 2) as	B	842	0.7			$S_{64}(99)$
γ(C=O) as	B	799	48.4	810/808/805/797	w	$S_4(11)$, $S_{29}(23)$, $S_{49}(14)$, $S_{62}(13)$
γ(C=O) s	A	782	15.5	785/783/780/777	w	$S_{28}(17)$, $S_{48}(21)$, $S_{61}(33)$
γ(C-H 1) as	B	716	38.6	724/720	m/m	$S_{29}(21)$, $S_{62}(60)$
ν(C-C)	A	713	39.3	716/713	m	$S_1(11)$, $S_{34}(21)$, $S_{61}(22)$
γ(C-H 1) s	A	689	50.2	693/689/688	m/sh/m	$S_{28}(14)$, $S_{34}(29)$, $S_{42}(10)$, $S_{61}(27)$
τ(ring 1) s	A	681	17.0	685/684	sh/m	$S_{36}(52)$, $S_{69}(24)$
τ(ring 1) as	B	681	11.4			$S_{37}(52)$, $S_{62}(15)$, $S_{70}(23)$
δ(C=O) as	B	643	107.5	646/645/642	S	$S_{35}(39)$, $S_{43}(12)$, $S_{45}(24)$
δ(ring 2) s	A	616	0.0	616	w	$S_{33}(88)$
δ(ring 2) as	B	616	1.4			$S_{33}(88)$
γ(ring) s	A	475	6.4	471	w	$S_{34}(12)$, $S_{38}(13)$, $S_{48}(28)$
γ(ring) as	B	451	3.7			$S_5(11)$, $S_{35}(18)$, $S_{39}(17)$, $S_{49}(24)$
δ(ring 3) as	B	422	0.4			$S_5(16)$, $S_{35}(20)$, $S_{39}(21)$, $S_{49}(18)$
δ(ring 3) s	A	413	0.0	n.i.		$S_4(11)$, $S_{34}(13)$, $S_{38}(19)$, $S_{48}(12)$
τ(ring 3) as	B	401	0.0			$S_{41}(72)$, $S_{68}(26)$
τ(ring 3) s	A	399	0.0			$S_{40}(66)$, $S_{67}(24)$
δ(CCC$_\alpha$) s	A	328	3.7			$S_1(23)$,$S_{28}(14)$,$S_{38}(10)$,$S_{42}(32)$,$S_{44}(15)$
ω(ring) as	B	271	32.5			$S_{43}(41)$, $S_{47}(42)$
ω(ring) s	A	260	0.1			$S_1(16)$, $S_4(13)$, $S_{46}(45)$
δ(C=O) s	A	154	0.2			$S_{38}(13)$, $S_{44}(32)$, $S_{46}(23)$
τ(ring 2) as	B	154	0.0	n.i.		$S_{39}(36)$, $S_{45}(10)$, $S_{47}(10)$, $S_{49}(20)$
τ(ring 2) s	A	145	2.4			$S_{28}(18)$, $S_{38}(23)$, $S_{48}(19)$, $S_{50}(17)$
δ(CCC$_\alpha$) as	B	125	1.4			$S_{73}(12)$, $S_{45}(27)$, $S_{47}(13)$, $S_{72}(20)$
τ(C-C_α) as	B	39	0.7			$S_{72}(78)$
τ(C-C_α) s	A	36	0.0			$S_{71}(92)$
τ(C-C)	A	26	2.4			$S_{50}(79)$

[a] Wavenumbers in cm^{-1}, calculated intensities in km mol^{-1}, ν, bond stretching, δ, bending, γ, rocking, ω, wagging, τ, torsion, n.i., not investigated. See Table S2 (Supporting Information) for definition of symmetry coordinates. Only approximated bands assigned to fundamental bands are presented in the table. [b] Scaled (0.978). [c] Only PED values greater than 10% are given. [d] Experimental intensities are presented in qualitative terms: S = strong; m = medium; w = weak; sh = shoulder; in some cases a single qualitative description is given for a group of overlapping bands assigned to the same vibration(s). [e] ν(C=O) vibrations are with all probability involved in Fermi resonance interactions with 2ν(C−C ring 1), 2γ(C−H 2) and the combination tones involving these two modes. [f] ν(C−C_α) is involved in Fermi resonance interaction with the overtones and combination tones associated with the bands whose fundamentals occur in the 620−760 cm^{-1} range. [g] Fermi resonance doublet.

calculated spectra regarding both frequencies and intensities. The assignments are presented in Table 1.

A noticeable feature of the infrared spectrum of matrix-isolated benzil is the multiplet structure and relative broadness of most of its bands. These characteristics are mainly a consequence of the conformational flexibility around the C−C central bond. As previously mentioned, the calculated frequency for the large-amplitude τC−C torsional vibration is as low as

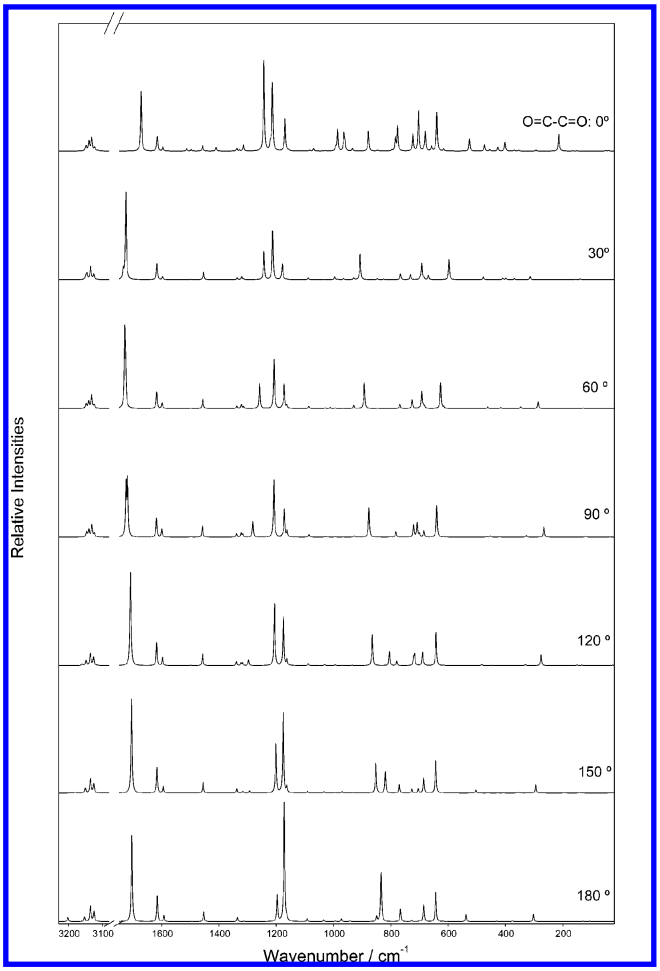

Figure 6. Calculated IR spectra as a function of the O═C−C═O dihedral angle. Calculated spectra were simulated using Lorentzian functions centered at the calculated (scaled) frequency with the bandwidth at half-height equal to 5 cm^{-1}.

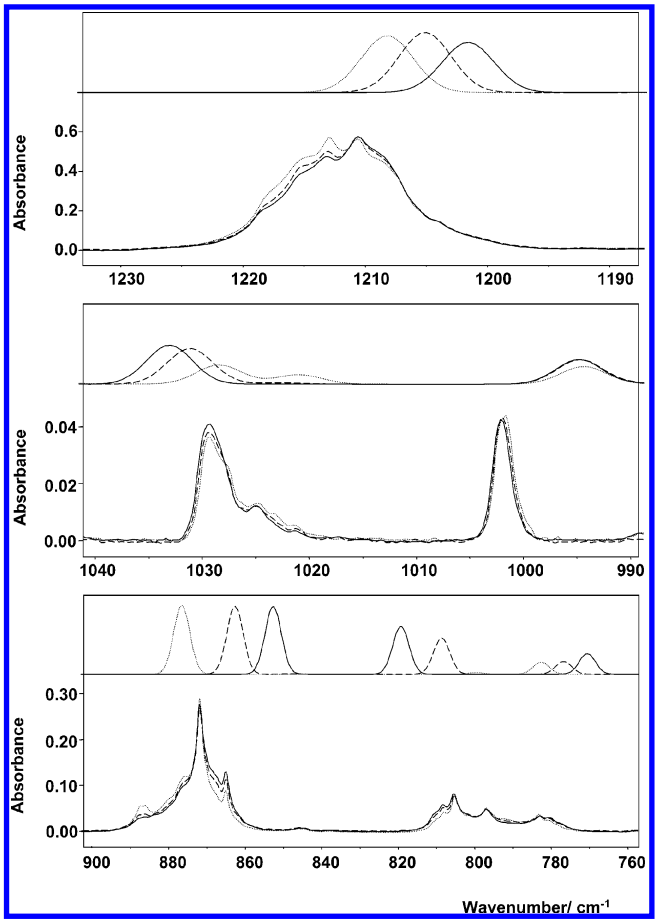

Figure 7. Selected spectral regions of the infrared spectra of benzil in an argon matrix showing the results of annealing experiments [—, as deposited (substrate temperature: 9 K); - - -, annealed at 26 K; ···, annealed at 34 K] and calculated spectra for different values of the O═C−C═O dihedral (···, 90°; - - -, minimum-energy conformation; —, 150°). Color versions of these pictures are also provided, together with analogous representations of other spectral regions, as Supporting Information, Figure S1. Calculated spectra were simulated using Lorentzian functions centered on the calculated (scaled) frequency with the bandwidth at half-height equal to 5 cm^{-1}.

26 cm^{-1} (even lower than that in diacetyl, which is 32 cm^{-1} [24]), and in the gas phase at the nozzle temperature (353 K), the fraction of molecules existing in thermodynamic equilibrium with a O═C−C═O dihedral angle that is significantly smaller or larger than its equilibrium value is substantial (Figure 3). The as-deposited matrix approximately retains the conformational distribution of the gas phase prior to deposition, and the observed spectrum shall then be a sum of contributions from all conformations that are significantly populated under those conditions. Figure 6 shows the dependence of the calculated infrared spectra of benzil on the O═C−C═O dihedral angle.[74] The spectral parameters (specially those associated with modes related to the O═C−C═O fragment) vary significantly with the conformation. Taking into consideration the fractional population curve for $T = 353$ K that is shown in Figure 3, it can be expected that conformations with a O═C−C−O dihedral angle ranging from ca. 90 to 150° contribute to the observed spectra in a significant manner. Then, to analyze the experimental data further, the calculated spectra for conformations with O═C−C═O dihedral angles of 90 and 150° will be considered to be reference spectra of molecules that have conformations closer to the cis and trans O═C−C═O arrangement than the minimum-energy conformation.

For a matrix-isolated molecule, the annealing of the matrix leads to conformational relaxation toward the most stable structure under these experimental conditions. As seen in Figure 3, the distribution of populations becomes very narrow at a temperature typical of a matrix. For benzil, it could be expected that annealing led to a decrease in the number of molecules with O═C−C═O dihedral angles both larger and smaller than the equilibrium angle, and as a result, the spectra should become narrower and show less-structured bands. Because the potential-energy profile predicted for a gas-phase molecule is slightly asymmetrical, growing faster near the minimum for larger angles, the total fractional population at $T = 353$ K slightly favors the molecules with O═C−C═O angles smaller than the minimum-energy conformation. Indeed, as previously shown, the energy-weighted average dihedral angle slightly decreases upon increasing the temperature of the gas, within the temperature limits considered in this study. Hence, we would expect that the annealing of the matrix would also reflect this fact and that when compared with the spectrum of the as-deposited matrix the spectrum of the annealed matrix gained similarity to the reference spectra of larger dihedral angle species (i.e., the depletion of the slightly more numerous molecules trapped in the matrix with smaller O═C−C═O dihedral angles than the equilibrium angle should be more pronounced than that of the molecules trapped with larger O═C−C═O dihedral angles). However, the experimental results do not follow the expectations extracted on the basis of a strict extrapolation of the gas-phase

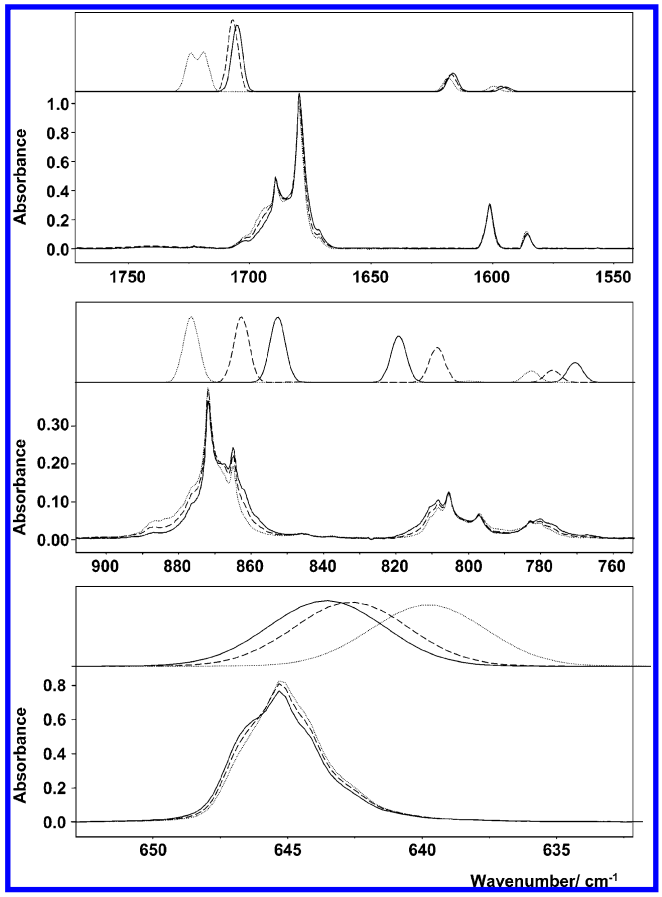

Figure 8. Selected spectral regions of the infrared spectra of benzil in an argon matrix showing the results of irradiation (λ > 235 nm) experiments [•••, as deposited (substrate temperature: 9 K); - - -, after 20 min of irradiation; —, after 417 min of irradiation] and calculated spectra for different values of the O═C−C═O dihedral (•••, 90°; - - -, minimum-energy conformation; —, 150°). Color versions of these pictures are also provided, together with analogous representations of other spectral regions, as Supporting Information, Figure S2. Calculated spectra were simulated using Lorentzian functions centered on the calculated (scaled) frequency with the bandwidth at half-height equal to 5 cm^{-1}.

torsional potential-energy profile for the matrix-isolated situation. In fact, the spectrum of the annealed matrix becomes more similar to the spectrum calculated for the species with smaller O═C−C═O angles (Figure 7[75]), thus indicating a decrease in the average dihedral angle. This result clearly reveals that the torsional potential changes in the matrix as a result of interactions with the matrix media, favoring more polar conformations with smaller O═C−C═O dihedral angles. The stabilization of more polar structures in matrixes, when compared with the gas phase, is a common phenomenon previously reported for various molecules with appreciable conformational flexibility.[69−71] This interpretation is also reinforced by PCM calculations, which predict that the O═C−C═O dihedral angle in the minimum-energy conformation of benzil in argon is ca. 80°, in agreement with results of previously reported semiempirical calculations.[6,30]

In a different experiment, irradiation of the matrix-isolated benzil was performed (λ > 235 nm). The results are summarized in Figure 8. (Data for other spectral regions are provided in Supporting Information, Figure S2.) As easily noticed, because irradiation leads to an increase in the average O═C−C═O dihedral angle, the spectra become more similar to the reference spectra that were calculated for conformations with larger O═C−C═O dihedral angles. Indeed, irradiation tends to push the molecule to a geometry closer to that of the lowest-energy conformation in the low-lying S_1 and T_1 electronic excited states. (As mentioned before, both are trans structures around the O═C−C═O axis.[6−17]) In agreement with the available data,[9] the benzil molecules should be preferentially photoexcited to the S_1 state and relax in this state toward its most stable trans planar geometry. For gaseous benzil molecules, the relaxation on the S_1 potential-energy surface should be barrierless.[6] However, in a matrix, it is inevitably hindered to some extent because of the steric constraints imposed by the solid environment. Intersystem crossing to the T_1 state and further conformational relaxation can eventually take place[9] before the transition back to the S_o state. The global result of this chain of processes is the spectroscopically probed change in the average O═C−C═O angle toward a larger value.

Conclusions

The low-temperature matrix-isolation FTIR spectroscopy study of benzil presented here, supported by extensive DFT calculations, enabled us to conclude that the low-frequency (ca. 26 cm^{-1}), large-amplitude torsion around the C−C central bond strongly affects the structural and spectroscopic properties exhibited by the compound. Besides the general assignment of the infrared spectrum of the matrix-isolated compound, it was shown that the equilibrium conformational distribution of molecules with different O═C−C═O dihedral angles existing in the gas phase and trapped in a low-temperature inert matrix can be changed toward a population where the average value of the O═C−C═O dihedral angle increases by irradiation with UV light (λ > 235 nm) or decreases by annealing the matrix to higher temperatures ($T \approx 34$ K). The effect of the annealing on the conformational populations can be explained by considering that more-polar conformations (corresponding to smaller O═C−C═O dihedral angles) are stabilized in the matrix compared with those in the gaseous phase as a consequence of the change in the S_o C−C torsional potential resulting from interactions with the matrix media. The effect of the UV irradiation can be explained in terms of conformational relaxation in the excited electronic states (S_1 and T_1), whose lowest-energy conformations correspond, in both cases, to a nearly planar configuration with the O═C−C═O dihedral angle equal to 180°.

Acknowledgment. This work was held under the POCTI/QUI/43366/2001 Research Program, FEDER, CONICET, and Agencia Nacional de Promoción Científica y Tecnológica-PICT 13080.

Supporting Information Available: Selected spectral regions of the infrared spectra of benzil in an argon matrix showing the results of annealing experiments and irradiation experiments, experimental and calculated bond lengths and angles, definition of internal symmetry coordinates used in the normal-mode analysis of benzil, and calculated wavenumbers, IR intensities, and potential-energy distributions for the C_2 conformer of benzil. This material is available free of charge via the Internet at http://pubs.acs.org.

References and Notes

(1) Miller, A. G.; Meade, S. J.; Gerrard, J. A. *Bioorg. Med. Chem.* **2003**, *11*, 843.

(2) Meade, S. J.; Miller, A. G.; Gerrard, J. A.*Bioorg. Med. Chem.* **2003**, *11*, 853.

(3) Kida, T.; Michinobu T.; Zhang, W.; Nakatsuji, Y.; Ikeda, I. *Chem. Commun. (Cambridge)* **2002**, *7*, 1596.

(4) Fan, X.; Subramaniam, R.; Weiss, M. F.; Monnier, V. M. *Arch. Biochem. Biophys.* **2003**, *409*, 274.

(5) (a) Martin, J. *Neues Jahrb. Mineral., Monatsh.* **2004**, *7*, 30. (b) Martin, J. *Z. Kristallogr.* **1891**, *21*, 139.
(6) Das, K.; Majumdar, D. *J. Mol. Struct.* **1993**, *288*, 55.
(7) Lacoge, N.; Buntinx, G.; Ratovelomanana, N.; Poizat, O. *J. Phys. Chem* **1992**, *96*, 1106.
(8) Singh, A.; Palit, D.; Mittal, J. *Chem. Phys. Lett.* **2002**, *360*, 443.
(9) Mizuno, M.; Iwata, K.; Takahashi, H. *J. Mol. Struct.* **2003**, *661*−*662*, 3.
(10) Fessenden, R.; Carton, P.; Shlmamori, H.; Scalano, J. *J. Phys. Chem.* **1982**, *86*, 3803.
(11) Asano, K.; Aita, S.; Azumi, T. *J. Phys. Chem.* **1984**, *88*, 5538.
(12) Roy, D.; Bhattacharyya, K.; Bera, S.; Chowdhury, M. *Chem. Phys. Lett.* **1980**, *69*, 134
(13) Chan, I.; Nelson, N. *J. Chem. Phys.* **1975**, *62*, 4080.
(14) Arnett, J.; McGlynn, S. *J. Phys. Chem.* **1975**, *79*, 626.
(15) Arnett, J.; Newkome, G.; Mattice; W.; McGlynn S. *J. Am. Chem. Soc.* **1974**, *96*, 4385.
(16) Morantz, D. J.; Wright, A. J. C. *J. Chem. Phys.* **1971**, *54*, 692.
(17) Bera, S.; Mukherjee, S.; Chowdhury M. *J. Chem. Phys.* **1969**; *51*, 754.
(18) Chattopadhyay, N.; Serpa, C.; Arnaut, L. G.; Formosinho, S. J. *Chem. Phys. Lett.* **2001**, *347*, 361.
(19) Jerphagon, J. *J. Quantum Electron.* **1971**, *QE*−*7*, 42.
(20) Brown, C. J.; Sadanaga, R. *Acta Crystallogr.* **1965**, *18*, 158.
(21) Cloizeaux, D. C. *Acad. Sci.* **1869**, *68*, 308.
(22) Gabe, E. J.; Le Page, Y.; Lee, F. L.; Barclay, L. R. C. *Acta Crystallogr., Sect.B* **1981**, *37*, 197.
(23) Shen, Q.; Hagen, K. *J. Phys. Chem.* **1987**, *91*, 1357.
(24) Gómez-Zavaglia, A.; Fausto R. *J. Mol. Struct.* **2003**, *661*−*662*,195.
(25) Smeyers, V.; Senent, M.; Peñavel, F.; Moule, D. *J. Mol. Struct.* **1993**, *287*, 117.
(26) Cureton, P.; Le Fèvre, C.; Le Fèvre, R. *J. Chem. Soc.* **1961**, 4447.
(27) Bloom, G.; Sutton, L. *J. Chem. Soc.* **1941**, 727.
(28) Volovšek, V.; Colombo, L. *J. Mol. Struct.* **1993**, *293*, 201.
(29) Volovšek, V.; Colombo, L. *J. Phys. Chem.* **1993**, *97*, 1283.
(30) Pawelka, Z.; Koll, A.; Zeegers-Huyskens, T. *J. Mol. Struct.* **2001**, *597*, 57.
(31) Tyrrell, J. *J. Mol. Struct.* **1992**, *258*, 41.
(32) Cumper, C.; Thurston, P. *J. Chem. Soc., Perkin Trans. 2* **1972**, 106.
(33) Bhattacharyya, K.; Chowdhury, M. *J. Photochem.* **1986**, *33*, 61.
(34) Hanuza, J.; Sąsiadek, W.; Kucharska, E.; Michalski, J.; Mączka, M.; Kaminskii, A.; Koronienko, A.; Dunina, E.; Klapper, H.; Hulliger, J.; Mohmed, A. *J. Raman Spectrosc.* **2004**, *35*, 224.
(35) Kolev, T. *J. Mol. Struct.* **1995**, *349*, 381.
(36) Kolev, T.; Jucjnovski, I. *Spectrosc. Lett.* **1993**, *26*, 1.
(37) Colombo, L.; Kirin, D.; Volovsek, V.; Lindsay, N. E.; Sullivan, J. F.; Durig, J. R. *J. Phys. Chem.* **1989**, *93*, 6290.
(38) Moore, D.; Tekippe, V.; Ramdas, A.; Toledano, J. *Phys. Rev. B* **1983**, *27*, 7676.
(39) Sapriel, J.; Boudou, A.; Perigaud, A. *Phys. Rev. B* **1979**, *19*, 1484.
(40) Juarez, M.; Lomas, M.; Bellanato, J. *Anal. Quim.* **1976**, *72*, 607.
(41) Claus, R.; Schrötter, H.; Brandmüller, J.; Haussühl, S. *J. Chem. Phys.* **1970**, *52*, 6448.
(42) Claus, R.; Hacker, H.; Schrötter, H.; Brandmüller, J. *Phys. Rev.* **1969**, *187*, 1128.
(43) Stenman, F. *J. Chem. Phys.* **1969**, *51*, 3141.
(44) Solin, S.; Ramdas, A. *Phys. Rev.* **1968**, *174*, 1069.
(45) Sterk, H. *Monatsh. Chem.* **1968**, *99*, 999.
(46) Chaudhuri, N.; El-Sayed, M. *J. Chem. Phys.* **1967**, *47*, 1133.
(47) Bernal, I. *Nature* **1963**, *200*, 1318.
(48) More, M.; Odou, G.; Levefre, J. *Acta Crystallogr.* **1987**, *B43*, 398.
(49) Zielinski, P.; More, M.; Cochon, E.; Lefebvre, J. *J. Chem. Phys.* **1996**, *104*, 3329.
(50) Bonno, B.; Laporte, J.; Rousset, Y. *Phys. Rev. B* **1991**, *43*, 12767.
(51) Yoshihara, A.; Yoshizawa, M.; Yasuda, H.; Fujimura, T. *Jpn. J. Appl. Phys.* **1985**, *24*, 367.
(52) Moore, D.; Tekippe, V.; Ramdas, A.; Toledano, J. *Phys. Rev. B* **1983**, *27*, 7676.
(53) Terauchi, H.; Kojima, T.; Sakaue, K.; Tajiri, F.; Maeda, H. *J. Chem. Phys.* **1982**, *76*,612.
(54) Kohda, K.; Nakamura, N.; Chihara, H. *J. Phys. Soc. Jpn.* **1971**, *51*, 2709.
(55) Moore, D.; Tekippe, V.; Ramdas, A.; Toledano, J. *J. Phys., Colloq.* **1981**, *42*, 785.
(56) Toledano, J. *Phys. Rev. B* **1979**, *20*, 1147.
(57) Odou, G.; More, M.; Warin, V. *Acta Crystallogr., Sect. A* **1978**, *34*, 459.
(58) Esherick, P.; Kohler, B. *J. Chem. Phys.* **1973**, *59*, 6681.
(59) Reva, I.; Stepanian, S.; Adamowicz, L.; Fausto, R. *J. Phys. Chem. A* **2001**, *105*, 4773.
(60) Lopes, S. B.; Lapinski, L.; Fausto, R. *Phys. Chem. Chem. Phys.* **2002**, *4*, 1014.
(61) Frisch, M. J.; Trucks, G. W.; Schlegel, H. B.; Scuseria, G. E.; Robb, M. A.; Cheeseman, J. R.; Zakrzewski, V. G.; Montgomery, J. A., Jr.; Stratmann, R. E.; Burant, J. C.; Dapprich, S.; Millam, J. M.; Daniels, A. D.; Kudin, K. N.; Strain, M. C.; Farkas, O.; Tomasi, J.; Barone, V.; Cossi, M.; Cammi, R.; Mennucci, B.; Pomelli, C.; Adamo, C.; Clifford, S.; Ochterski, J.; Petersson, G. A.; Ayala, P. Y.; Cui, Q.; Morokuma, K.; Malick, D. K.; Rabuck, A. D.; Raghavachari, K.; Foresman, J. B.; Cioslowski, J.; Ortiz, J. V.; Stefanov, B. B.; Liu, G.; Liashenko, A.; Piskorz, P.; Komaromi, I.; Gomperts, R.; Martin, R. L.; Fox, D. J.; Keith, T.; Al-Laham, M. A.; Peng, C. Y.; Nanayakkara, A.; Gonzalez, C.; Challacombe, M.; Gill, P. M. W.; Johnson, B. G.; Chen, W.; Wong, M. W.; Andres, J. L.; Head-Gordon, M.; Replogle, E. S.; Pople, J. A. *Gaussian 98*, revision A.9; Gaussian, Inc.: Pittsburgh, PA, 1998.
(62) Becke, A. D. *Phys. Rev. A* **1988**, *38*, 3098.
(63) Lee, C. T.; Yang, W. T.; Parr, R. G. *Phys. Rev. B* **1988**, *37*, 785.
(64) Csaszar, P.; Pulay, P. *J. Mol. Struct.*: *THEOCHEM* **1984**, *114*, 31.
(65) Schachtschneider, J. H. Technical Report; Shell Development Co.: Emeryville, CA, 1969.
(66) Miertus, S.; Scrocco, E.; Tomasi, J. *Chem. Phys.* **1981**, *55*, 117.
(67) Danielson, D.; Helberg, K. *J. Am. Chem. Soc.* **1979**, *101*, 3730.
(68) Wong, M.; Frisch, M.; Wiberg, K. *J. Am. Chem. Soc.* **1991**, *113*, 4776.
(69) Reva, I. D.; Ilieva, S. V.; Fausto, R. *Phys. Chem. Chem. Phys.* **2001**, *3*, 4235.
(70) Lopes, S.; Lapinski, L.; Fausto, R. *Phys. Chem. Chem. Phys.* **2002**, *4*, 5952.
(71) Reva, I. D.; Stepanian, S. G.; Adamowicz, L.; Fausto, R. *Chem. Phys. Lett.* **2003**, *374*, 361.
(72) Benzil is also known as bibenzoyl, dibenzoyl, diphenylethanedione, diphenylglyoxal, 1,2-diphenylethane-1,2-dione, 1,2-diphenylethanedione, and diphenyl-α,β-diketone.
(73) To do this calculation on the basis of the classical model described above in this paper, it is necessary to replace $|\alpha|$ in eq 1 by $|\mu|$, where μ is the dipole moment. (Note that because of the symmetry of the molecule the alignment of the dipole moment is always the same.)
(74) The results given in Figure 6 were obtained with the smaller 6-31G(d,p) basis set; however, the spectra obtained with this basis set and with the larger 6-311++G(d,p) basis set for the minimum-energy conformation were found to be practically equal; the same can be expected to occur for other conformations.
(75) Data referring to other spectral regions not shown in Figure 7 are provided as Supporting Information, Figure S1.